Journal of Nuclear Materials 390–391 (2009) 339–342

Contents lists available at ScienceDirect

Journal of Nuclear Materials

journal homepage: www.elsevier.com/locate/jnucmat

Spatial structure of scrape-off-layer filaments near the midplane and X-point regions of Alcator-C-Mod

J.L. Terry [a,*], S.J. Zweben [b], M.V. Umansky [c], I. Cziegler [a], O. Grulke [d], B. LaBombard [a], D.P. Stotler [b]

[a] Plasma Science and Fusion Center, MIT, 175 Albany St., Cambridge, MA 02139, USA
[b] Princeton Plasma Physics Laboratory, Princeton, NJ 08543, USA
[c] Lawrence Livermore National Laboratory, Livermore, CA 94550, USA
[d] Max Planck Institute for Plasma Physics, Greifswald, Germany

ARTICLE INFO

PACS:
52.35.Ra
52.30.−q
52.55.−Fa
52.70.Kz

ABSTRACT

Movies of edge turbulence at both the outboard midplane and the region outboard of the typical lower X-point location in C-Mod have been obtained using gas-puff-imaging together with fast-framing cameras. Intermittent turbulence structures, typically referred to as blobs or filaments, are observed in both locations. Near the midplane the filaments are roughly circular in cross-section, while in the X-point region they are highly elongated. Filament velocities in this region are ~3x faster than the radial velocities at the midplane, in a direction roughly outward across the local flux surfaces. The observations are consistent with the picture that the filaments arise in the outboard region and, as a consequence of the rapid parallel diffusion of the potential perturbations, map along field lines. Results from a 3D BOUT turbulence simulation reproduce many of the spatial features observed in the experiment.

1. Introduction

There is great interest, both experimental and theoretical, in the intermittent convective transport that is routinely observed in the far scrape-off-layer (SOL) on the outboard 'bad-curvature' side of tokamak plasmas. This convective transport dominates the perpendicular particle transport in the far-SOL [1]. The interest in it derives primarily from its impact on crucial reactor issues like density-scale-length in the far-SOL, divertor design, wall-recycling, and the physics of the density limit. Most previous experimental studies have measured characteristics of this transport phenomenon in the outboard *midplane* region. It is the purpose of this work to present and discuss some of the characteristics of the turbulence structures responsible for the convective transport in regions *away* from the outboard midplane, in particular, in the region outboard of the lower X-point, and to relate them to characteristics of the turbulence structures in the midplane region. These turbulence structures are typically referred to in the literature as filaments or blobs or mesoscale structures. Our choice to view the X-point region was made primarily for two reasons: (1) we wanted to get as close as was practical to the X-point in order to investigate the effects on the filaments (if any) of the flux expansion and magnetic shearing that occurs when moving along field lines to the X-point region, and (2) we wanted to be able to distinguish whether the primary filament motion there is normal to the local flux surfaces or is in the major radius direction, since in the midplane region these directions are the same.

2. Experimental details

Prior to this study, turbulence imaging diagnostics on C-Mod viewed only the outboard and inboard midplane regions (Fig. 1). One view of the outboard midplane covers a 6 cm × 6 cm region and is approximately parallel to the field. The 2D images of this view are registered using a fast-framing camera [2]. Viewing parts of the same region are two linear arrays of views, one radial and the other vertical, that are coupled to filtered photodiodes and sampled at a 1 MHz rate. Viewing the inboard midplane region is another radial array. These views are close to gas puff nozzles that provide a toroidally-localized source of deuterium, whose D_α emissions respond to local n_e and T_e fluctuations and are detected by the optical diagnostics (so-called gas-puff-imaging, GPI [3]). These nozzles are typically ~1–3 cm from the local separatrix and at the edges of the views themselves. To complement these diagnostics, we installed a new view of the region just outboard of the location of the typical lower X-point for the reasons stated above. (For brevity we will hereafter refer to this as the 'Xpt view' or the 'Xpt region', even though it does not actually view the X-point.) This ~6 cm × 6 cm view is also approximately along the local field. A nozzle embedded in the divertor structure under the view provides the local gas puff. This nozzle is ~3 cm below the bottom

* Corresponding author.
E-mail address: terry@psfc.mit.edu (J.L. Terry).

0022-3115/$ - see front matter © 2009 Elsevier B.V. All rights reserved.
doi:10.1016/j.jnucmat.2009.01.152

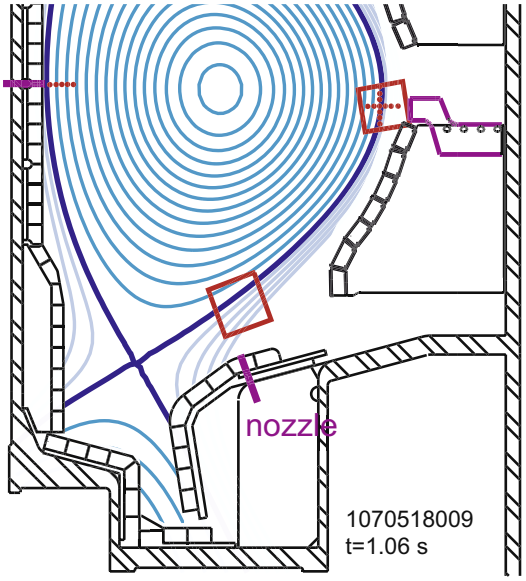

Fig. 1. Poloidal X-section of a DN C-Mod discharge, showing the turbulence imaging diagnostics: the 2D 'Xpt view', outboard of the lower X-pt (red square); the 2D view at the outboard midplane (red square) with the radial and vertical arrays of diode-coupled views (red dots); and the radial array of views at the inboard midplane (red dots). For the GPI, gas is puffed from the 3 nozzles (purple). (For interpretation of the references to color in this figure legend, the reader is referred to the web version of this article.)

of the view, ~6 cm from the view center, and ~7–9 cm below the typical separatrix location. The view is separated toroidally from the viewed outboard midplane region, and the two regions are not connected along magnetic field lines. All views are shown in Fig. 1. Movies of edge turbulence in the Xpt region and at the midplane are obtained using fast-framing (150 000 frame/s) cameras. While, for this study, movies from both views were not recorded simultaneously, the outboard midplane 'diode-views' were recorded simultaneously with the movies at each location. For analysis of the images of the Xpt region, plasmas in DN, USN, or limited configuration were used, since in those configurations emission from the local puff was much greater than the intrinsic D_α emission (as is necessary in order to localize the measurement).

3. Comparisons of filament characteristics – outboard midplane vs Xpt region

As has been previously reported (see Ref. [4] and references therein), turbulence in the outboard far-SOL of C-Mod and most other tokamaks is intermittent. Distributions in the fluctuation magnitudes of various measured quantities (like local GPI emission, I_{sat}, and V_{float}) are strongly skewed toward larger magnitude fluctuations. Imaging at the outboard midplane in the vertical-toroidal plane shows that the turbulent fluctuations have a filamentary structure, aligned with the local field and with $k_{||} \ll k_{perp}$ (e.g. [5,6]). When these filaments are viewed in a vertical-radial plane at the midplane, along chords parallel to the local field, their cross-sections are roughly circular in shape with a characteristic diameter (correlation length) of ~1 cm [7]. Images from the outboard midplane view illustrating this can be found in Ref. [8]. In the SOL of the outboard midplane the filaments move both radially and poloidally at speeds up to ~1000 m/s [9]. Fluctuations at the inboard midplane are much reduced, both in absolute and relative magnitude [8,10]. Filaments are not observed there.

Imaging at the Xpt region also shows intermittent fluctuations. The cross-sectional shape of the turbulence structures as imaged with GPI, however, is much different than at the midplane. Highly-elongated cross-sections – 'fingers' – are observed, as illustrated in a single frame from this view and shown in Fig. 2. In the lower-left part of the view, the long dimension of the fingers is typically tilted by angles of up to ~45° below horizontal. Motions of the fingers there are primarily outward across flux surfaces (i.e. approximately perpendicular to the separatrix, also shown in Fig. 2) with speeds ~3x the radial speeds of the filament at the midplane (as determined by the time-delay cross-correlation method described in [9]). In the upper-right part of the view, the fingers' major axes are typically close to horizontal. Analyses of the Xpt region movies and of the simultaneously-measured outboard midplane 'diode view' time-signals yield profiles of auto-correlation times for the fluctuations, $\tau_{auto}(\rho)$, that are the same (within the scatter). (ρ is the distance outside the separatrix when mapped to the outboard midplane.) For DN discharges τ_{auto} is typically ~30 μs just inside the separatrix, falling to 15–20 μs at $\rho \gtrsim 1.5$ cm. Thus the auto-correlation times of the fluctuations, due primarily to the filament motion, are approximately the same in both regions.

The observations described above are reconciled within the following physical picture: filaments of high density plasma are generated primarily in the outboard, bad-curvature region. This is directly or indirectly related to the strong ballooning-like particle transport that occurs there, as implied by other measurements, e.g. the observed SOL flows [11], and consistent with the relatively small level of turbulence at the inboard midplane. Once the filaments are generated, we expect the basic model for filament motion, first elaborated in Ref. [12]: since the parallel conductivity of the plasma is large, perturbed electrostatic potentials inside a filament arising from curvature and $B\times\nabla\cdot B$ drifts are transmitted rapidly along magnetic field lines. The filament is thus polarized in a way that depends upon the integration of the cross-field polarization currents along the filament's length. A parallel diffusion coefficient for potential fluctuations, $D_\varphi \sim \sigma_{||}\ 4\pi V_{alfven}^2/(c^2 k_{perp}^2)$, can be derived from the current continuity equation, $\nabla\cdot j = 0$. Evaluation of this parallel diffusion coefficient yields the result that any potential perturbation will be communicated between the midplane and Xpt regions in C-Mod on the fast time scale of ~0.1 μs (for $B_t = 4$ T, $n_e = 3\times10^{19}$ m^{-3}, $T_e = 25$ eV, $k_{perp} = 200$ m^{-1}, $\lambda_{||} = 3$ m) [13]. Thus we expect that the rapid parallel propagation of potential gives rise to field-aligned filaments whose large-scale ($k_{perp}\rho_s \lesssim 0.04$) features map along field lines and whose drive

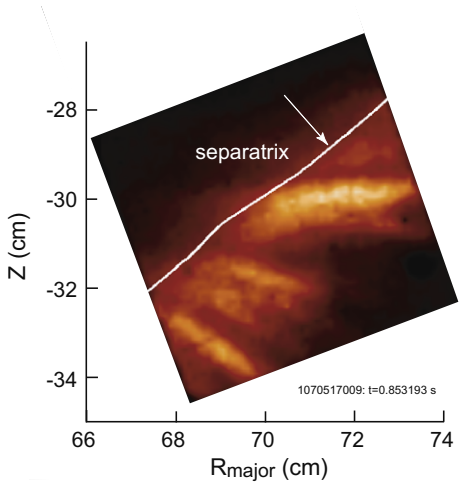

Fig. 2. A single movie image (2 μs exposure) from the Xpt view of a DN plasma showing the cross-sections of typical SOL filaments. The separatrix is also shown (white line). The gas is puffed from below the image.

and damping responses are integrated over at least part of the field line length.

Previous measurements on a stellarator [5] directly support this picture. Also previous cross-correlation measurements made on C-Mod by diagnostics separated by ~3 m along a field line [6] are consistent with the model presented above in that: (1) parallel correlation of density fluctuations was observed, and (2) the measured dipole structure of cross-correlations of potential fluctuations in the Xpt region was consistent with the measured size and outward propagation of the density fluctuations at the midplane.

This picture thus predicts that large-scale cross-field features of the filaments should magnetically map between the midplane region and the X-pt region. Indeed, the circular cross-sections of the filaments at the midplane do map into cross-sections in the Xpt region that are highly elongated and tilted (i.e. fingers), as observed. We have performed this mapping in detail for specific shots. Flux tubes that are circular (1 cm diameter) in cross-section at the midplane i.e. the rough size and shape of the filament cross-sections observed in the midplane region, are mapped to the Xpt view, where they are approximately ellipsoidal in cross-section, having been stretched by flux expansion and tilted by shearing. We have quantitatively compared the tilts of these mapped flux tubes with the tilts of the observed fingers and compared the lengths of the major diameters of the mapped flux tubes with the correlation lengths of the fluctuations along the finger tilt axes. The observed tilt angles are determined by finding (at any point in the image) the angle of the line for which the line-integrated cross-correlation of the reference location and the rest of the image is maximum. The correlation length along this line is then calculated. Typically ~300 sequential images are used for these determinations. Results from such a comparison are shown in Fig. 3, where the black bars represent the lengths and tilts of the major axes of the 1-cm-mapped-flux-tubes. The alignment of red bars represents the *measured* tilt angles, while the lengths of the red bars are proportional to the *measured* correlation lengths, determined as described above. There is typically good agreement in the tilt angles in the lower-left section of the experimental view. The measured finger correlation lengths there are within a factor of 2 of the flux tube major diameters, also in good agreement, given the quantities being compared. In the lower part of the view, we find approximate agreement with the mapping model in DN, USN, and limited configurations; thus the finger structure does not depend upon nearness to a primary X-point.

However, a major and obvious inconsistency between the flux-tube-mapping model and the observations is the disagreement between finger tilts and finger lengths observed in the upper portion of the images and those predicted by the mapping model. The fingers in the upper portion of the view are typically nearly horizontal and 2–5 cm in length, while the mapping predicts tilts of $-10°$ to $-35°$ with flux tube major diameters of ~1.6 cm. We attribute this discrepancy to a limitation of the gas-puff-imaging in the upper-right portion of the view. The discrepancy arises essentially because the toroidal extent of the puff-gas cloud is too large there and because emission *along* a field line will appear in the image as a nearly horizontal line. Modeling of the view and its puff with the 3D neutrals code DEGAS2 [14] indicates that the toroidal FWHM of the emission from the puff is ~10 cm at the center of the view, increasing to 15–20 cm at the top of the view. (These extents are larger for the Xpt view because its nozzle is significantly further from the view than for the midplane views.) Modeling the effects of filament emission with different toroidal extents shows that, if the extent is 20 cm, a filament of very small cross-section will be imaged as a *horizontal* line of ~2 cm length. If this effect is convolved over the cross-section expected for the filament from magnetic mapping, then correlation lengths are longer and finger tilt angles are more horizontal than those of the mapped filament

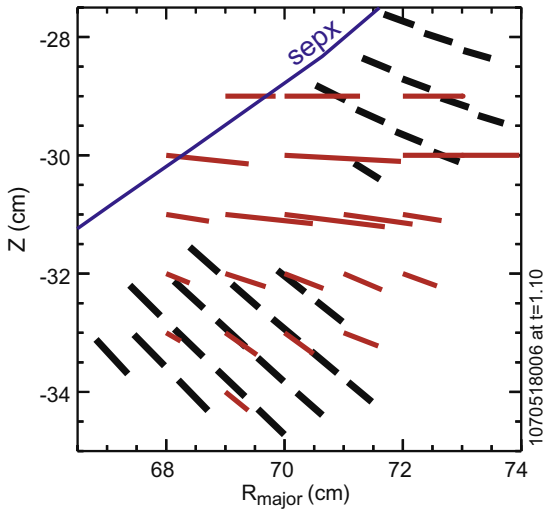

Fig. 3. Comparison between measured finger tilts and lengths and those predicted by mapping 1 cm diameter flux tubes from the midplane to the viewing location. The angles for which the line integral cross-correlation values in the movie images are maximum are shown by the red bars, whose lengths are proportional to the fluctuation correlation lengths along that line. The angles and lengths of the major axes of the mapped flux tubes are shown by the black bars. The actual correlation lengths and major diameters are 2.86x longer than shown, but are scaled in the figure for clarity. (For interpretation of the references to color in this figure legend, the reader is referred to the web version of this article.)

cross-sections, as is observed in the upper part of the images. It is probable that this effect is playing a significant role in the observations in the upper portion of the image and is the primary reason for the disagreement with the mapping there. Since the toroidal extent of the cloud in the lower part of the view is predicted to be ~5 cm, this effect should be and appears to be small there.

The flux-tube-mapping model also predicts that the cross-field velocities should be roughly normal to the local flux surfaces and be roughly proportional to the radial flux expansion ratio between the two viewed regions; since the filament cross-sections map with the flux tubes, the poloidal dimension of the filament will be reduced by approximately the same ratio, thereby increasing E_{pol} in the $E_{pol}xB$ drive. Quantitatively, velocities normal to the flux surfaces in the Xpt region that are ~3x faster than the midplane radial velocity are expected, roughly what we observe. This result has not been tested more quantitatively since simultaneous imaging of the same flux tube at the two locations has not been done. We also note that any blurring of images due to this motion and the frame integration time ($\leqslant 4$ μs) is significantly less than the long dimension of filament cross-sections in the images. Finally, we note that many aspects of the flux-tube-mapping of filaments have been discussed theoretically [13,15,16] before knowledge of these experimental results.

4. Comparisons with turbulence simulation results

Aspects of the spatial structure of the filamentary SOL turbulence have been examined using the BOUT 3D non-linear simulation code [17]. BOUT uses a system of reduced Braginskii fluid equations in realistic flux tube geometry, including X-point effects. For this simulation, turbulence in a flux tube domain (whose cross-section at the outboard midplane is 2 cm radially × 4 cm poloidally) is simulated for a C-Mod EFIT equilibrium with measured SOL profiles of n_e and T_e. Filaments of approximately the same size scale as in the experiments, i.e. features of ~1 cm cross-sectional size, appear at the midplane, although additional fine scale structure is present in the simulation that is not resolved in the experiment.

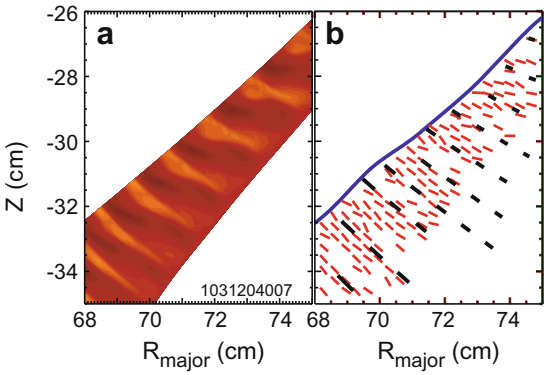

Fig. 4. (a) The ion density fluctuation at one instant within the Xpt region from the BOUT simulation, showing multiple poloidal cuts of a typical filament (see text). (b) Comparison of the tilt angles of the filament cross-sections in the simulation (red bars) and the tilt angles of the major axes of the mapped flux tubes (black bars). The lengths of the black bars are proportional to the lengths of flux tube major axes. The lengths of the simulation fingers were not found, since the correlation lengths along the tilt angles extended outside the simulation domain. Thus all of the red bars are the same length. (For interpretation of the references to color in this figure legend, the reader is referred to the web version of this article.)

Since the Xpt view of the experiment is much larger than a single poloidal cut of the simulation flux tube domain at this location, the toriodal periodicity in the simulation is used to fill the viewed region by mapping multiple poloidal cuts to a single plane at constant toriodal angle. This results in different cuts of the same filament appearing in each frame of the simulation realization, as seen in Fig. 4(a), where the fluctuation ion density in the Xpt view is shown. It is clear that in this region the simulation filament cross-sections are tilted and elongated. Using the same analysis techniques that were used to determine the finger tilt angles for the experimental images, tilt angles for the simulation fingers were determined. As was done for the comparison with experimental tilt angles in Fig. 3, the simulation tilt angles (red bars) were compared with those of flux tubes that were magnetically mapped from circularly cross-sectioned flux tubes at the midplane (black bars). The result is shown in Fig. 4(b), where on average the angles of the long dimensions of the filament cross-sections in the simulation match quantitatively the magnetic mapping. This indicates that the magnetic mapping of features with $k_{perp}\rho_s \sim 0.02$ is also observed in the BOUT simulation.

5. Discussion and summary

We have studied the spatial structure and the parallel dynamics of the plasma filaments that appear routinely in the far-SOL of Alcator-C-Mod plasmas and are responsible for the bulk of the particle transport there. By imaging these filaments in the outboard midplane region and in the region of outboard of the lower X-point, we find that their cross-sections are roughly circular at the midplane, but are elongated into finger-like shapes in the Xpt region. The elongated and sheared cross-sections of the filaments observed in the lower part of the Xpt view are quantitatively consistent with a magnetic mapping of roughly circular cross-sectioned structures at the midplane region. These features are also reproduced in a simulation using the BOUT turbulence code. Furthermore, the fingers in the lower part of the Xpt view move outward approximately normal to flux surfaces with speed roughly 3x the outward radial velocities observed near the midplane. Thus we have provided measurements of the cross-sectional shapes of the filaments and their cross-field dynamics at two locations and discussed a model that can explain many of the observed features. In the model, rapid parallel diffusion of potential perturbations results in the magnetic mapping of filamentary structures. Such a mapping is quantitatively consistent with the observations. Results consistent with these, as well as similar conclusions, have also been published in Ref. [5], in which probe measurements of SOL fluctuations in W7-AS stellarator plasmas were analyzed.

There are a number of implications from this picture both for transport in the main chamber and for transport and dynamics in the divertor. Continued magnetic shearing and flux expansion close to the X-point may have important consequences for parallel and perpendicular transport, both because of their effects on the parallel extent [15] and stability of the filament and because, if the mapping continues to hold, the filaments are deformed into shapes where the poloidal scale length approaches the ion gyro-radius [18]. Whether the filaments cross the X-point region into the divertor is still unknown. If they do or if they arise in the divertor plasma, there exist possibilities for manipulating them and their effects on the divertor plasma, as discussed in detail in Refs. [19,18].

Acknowledgements

We would like to acknowledge valuable discussions with D. Ryutov and R. Cohen of Lawrence Livermore Laboratory and T. Stoltzfus-Dueck and J. Kommes of PPPL. This work is supported by DoE Coop. Agreement DE-FC02-99-ER54512 (MIT) and Contract Nos. DE-AC02-76CHO3073 (PPPL) and DE-AC52-07NA27344 (LLNL).

References

[1] L. Rudakov, J.A. Boedo, R.A. Moyer, et al., Plasma Phys. Control. Fus. 44 (2002) 717.
[2] J.L. Terry, B. LaBombard, B. Lipschultz, et al., Fus. Sci. Technol. 51 (2007) 342.
[3] J.L. Terry, R. Maqueda, C.S. Pitcher, et al., J. Nucl. Mater. 290 (2001) 757.
[4] S.J. Zweben, J.A. Boedo, O. Grulke, et al., Plasma Phys. Control. Fus. 49 (2007) 1.
[5] J. Bleuel, M. Endler, H. Niedermeyer, et al., New J. Phys. 4 (2002) 38.1.
[6] O. Grulke, J.L. Terry, B. LaBombard, et al., Phys. Plasma 13 (2006) 012306.
[7] S.J. Zweben, D.P. Stotler, J.L. Terry, et al., Phys. Plasma 9 (2002) 1981.
[8] J.L. Terry, S.J. Zweben, K. Hallatschek, et al., Phys. Plasma 10 (2003) 1739.
[9] J.L. Terry, S.J. Zweben, O. Grulke, et al., J. Nucl. Mater. 337–339 (2005) 322.
[10] B. LaBombard, J.E. Rice, A.E. Hubbard, et al., Nucl. Fus. 44 (2004) 1047.
[11] B. LaBombard, J.E. Rice, A.E. Hubbard, et al., Phys. Plasma 12 (2005) 056111.
[12] S.I. Krasheninnikov, Phys. Lett. A 283 (2001) 368.
[13] This 0.1 μs time scale is to be compared to the timescale for transport of density perturbations along the field between midplane and Xpt regions of $\lambda_{||}/C_s \sim 100$ μs.
[14] D.P. Stotler, J. Boedo, B. LeBlanc, et al., J. Nucl. Mater. 363–365 (2007) 686.
[15] J.R. Myra, D.A. D'Ippolito, Phys. Plasma 12 (2005) 092511.
[16] D.D. Ryutov, Phys. Plasma 13 (2006) 122307.
[17] X.Q. Xu, R.H. Cohen, G.D. Porter, et al., Nucl. Fus. 40 (2000) 731.
[18] D.D. Ryutov, R.H. Cohen, Contrib. Plasmas Phys. 48 (2008) 48.
[19] R.H. Cohen, B. LaBombard, D.D. Ryutov, et al., Nucl. Fus. 47 (2007) 612.